◆ Human Brain Mapping 36:4272–4286 (2015) ◆

G-Protein Genomic Association With Normal Variation in Gray Matter Density

Jiayu Chen,[1] Vince D. Calhoun,[1,2] Alejandro Arias-Vasquez,[3,4,5] Marcel P. Zwiers,[6] Kimm van Hulzen,[3] Guillén Fernández,[4] Simon E. Fisher,[7,8] Barbara Franke,[3,5] Jessica A. Turner,[1,9,10] and Jingyu Liu[1,2]*

[1]*The Mind Research Network, Albuquerque, New Mexico*
[2]*Department of Electrical and Computer Engineering, University of New Mexico, Albuquerque, New Mexico*
[3]*Department of Human Genetics, Radboud University Medical Centre, Donders Institute for Brain, Cognition and Behaviour, Nijmegen, The Netherlands*
[4]*Department of Cognitive Neuroscience, Radboud University Medical Centre, Donders Institute for Brain, Cognition and Behaviour, Nijmegen, The Netherlands*
[5]*Department of Psychiatry, Radboud University Nijmegen Medical Centre, Donders Institute for Brain, Cognition and Behaviour, Nijmegen, The Netherlands*
[6]*Centre for Cognitive Neuroimaging, Radboud University Nijmegen, Donders Institute for Brain, Cognition and Behaviour, Nijmegen, The Netherlands*
[7]*Language and Genetics Department, Max Planck Institute for Psycholinguistics, Nijmegen, The Netherlands*
[8]*Centre for Neuroscience, Radboud University Nijmegen, Donders Institute for Brain, Cognition and Behaviour, Nijmegen, The Netherlands*
[9]*Psychology Department, Georgia State University, Atlanta, Georgia*
[10]*Neuroscience Institute, Georgia State University, Atlanta, Georgia*

Abstract: While detecting genetic variations underlying brain structures helps reveal mechanisms of neural disorders, high data dimensionality poses a major challenge for imaging genomic association studies. In this work, we present the application of a recently proposed approach, parallel independent component analysis with reference (pICA-R), to investigate genomic factors potentially regulating gray matter variation in a healthy population. This approach simultaneously assesses many variables for an aggregate effect and helps to elicit particular features in the data. We applied pICA-R to analyze gray matter density (GMD) images (274,131 voxels) in conjunction with single nucleotide polymorphism (SNP) data (666,019 markers) collected from 1,256 healthy individuals of the Brain Imaging Genetics (BIG) study. Guided by a genetic reference derived from the gene *GNA14*, pICA-R identified a signifi-

Additional Supporting Information may be found in the online version of this article.

Contract grant sponsor: National Institutes of Health; Contract grant number: 1R01MH094524; Contract grant sponsor: European Community's Seventh Framework Programme (FP7/2007–2013); Contract grant number: 278948; 602450.

*Correspondence to: Jiayu Chen, The Mind Research Network 1101 Yale Blvd. NE. Albuquerque, NM, USA 87106-3834. E-mail: jchen@mrn.org

Received for publication 2 February 2015; Revised 8 July 2015; Accepted 14 July 2015.

DOI: 10.1002/hbm.22916
Published online 7 August 2015 in Wiley Online Library (wileyonlinelibrary.com).

cant SNP-GMD association ($r = -0.16$, $P = 2.34 \times 10^{-8}$), implying that subjects with specific genotypes have lower localized GMD. The identified components were then projected to an independent dataset from the Mind Clinical Imaging Consortium (MCIC) including 89 healthy individuals, and the obtained loadings again yielded a significant SNP-GMD association ($r = -0.25$, $P = 0.02$). The imaging component reflected GMD variations in frontal, precuneus, and cingulate regions. The SNP component was enriched in genes with neuronal functions, including synaptic plasticity, axon guidance, molecular signal transduction via PKA and CREB, highlighting the *GRM1*, *PRKCH*, *GNA12*, and *CAMK2B* genes. Collectively, our findings suggest that *GNA12* and *GNA14* play a key role in the genetic architecture underlying normal GMD variation in frontal and parietal regions. *Hum Brain Mapp 36:4272–4286, 2015.*

Key words: SNP; sMRI; multivariate; semi-blind; G-protein

INTRODUCTION

Studying associations between genetic variables and imaging traits is a valuable strategy, a maturing field known as imaging genetics, which holds the promise to help better understand the genetic underpinnings of cognition and reveal biological mechanisms of mental disorders [Thompson et al., 2014]. Structural magnetic resonance imaging (sMRI) provides a noninvasive approach to study the morphology of the living brain. Quantitative measures are derived from T_1-weighted MRI images using computational methods such as voxel-based morphometry (VBM) [Ashburner and Friston, 2005] or cortical surface reconstruction (FreeSurfer) [Fischl and Dale, 2000] to depict various structural features, including brain volume, gray matter volume, cortical thickness, and surface area. These features can then be compared at subject level for their functional implications. Under this strategy, biomarkers have been consistently identified from both healthy and diseased human brains, characterizing neural development, ageing, Alzheimer's disease, schizophrenia, and so on [Ellison-Wright et al., 2008; Frisoni et al., 2010; Giedd and Rapoport, 2010; Raz and Rodrigue, 2006]. More importantly, many attributes of brain structure, including both global and regional traits, are confirmed to be genetically influenced in twin studies, with heritability estimated around 40–90% [Peper et al., 2007; Thompson et al., 2001; Winkler et al., 2010].

Heterotrimeric guanine nucleotide-binding proteins (G-proteins) serve as molecular switches in intracellular singling cascades, where they sense signals from cell-surface receptors that are activated by extracellular stimuli and transduce signals to downstream effectors [Oldham and Hamm, 2008]. It has been documented that activated G-proteins directly interact with a variety of effector proteins, including phosphodiesterase E, phospholipase D, phospholipase C, inducible nitric oxide synthase, calcium channels, and the G protein-regulated inducer of neurite outgrowth 1 and 2 [Cabrera-Vera et al., 2003]. Particularly, G-proteins are richly expressed in the brain and involved in cortical development, neuronal growth as well as neuronal signaling [Bromberg et al., 2008; Hamm, 1998; Offermanns, 2001]. For instance, there is evidence that G protein alpha 12 and alpha 13 can mediate growth cone collapse and neurite retraction [Nurnberg et al., 2008], while deficiency of the G-protein α-subunits causes localized overmigration of neurons in the developing cerebral and cerebellar cortices [Moers et al., 2008]. Knockout of G protein beta 5 impairs brain development and causes multiple neurologic abnormalities in mice [Zhang et al., 2011]. Neural expression of G protein-coupled receptor 3, 6, and 12 has been implicated in up-regulating cyclic AMP (cAMP) levels in neurons and stimulating neurite outgrowth [Tanaka et al., 2007].

Given their roles in neural development, G-proteins pose promising candidates for imaging genetic association studies. More recently, Chavarria-Siles et al. [2013] investigated 502 single nucleotide polymorphisms (SNPs) in 25 G-protein genes for their associations with brain-wide gray matter volume using a mass univariate model. They identified seven SNPs to be significantly associated with gray matter volume variation in different brain regions, including the medial frontal cortex. While this work provides direct evidence that G-protein SNPs are related to brain structure, the univariate analysis is not able to assess the aggregate effects of multiple variants. In addition, considering that G-proteins are key cell signaling molecules and affect multiple biological processes, their effect on neurobiological conditions is likely not isolated but involves a large network. Therefore, a multivariate study is strongly encouraged to search for G-protein involved genetic components that may better delineate the basis of the gray matter variation.

In the present work, we applied a semi-blind multivariate approach, parallel independent component analysis with reference (pICA-R) [Chen et al., 2013], to explore G-protein involved genomic factors underlying brain structure in a large homogeneous cohort of 1,256 healthy Caucasians. Brain-wide gray matter density (GMD) images were analyzed in conjunction with genome-wide SNP data. G-proteins identified in the work by Chavarria-Siles et al. [2013] served as references to guide the analysis but

TABLE I. Summary of BIG scanning parameters

Scanning parameter	Variations across subjects
Station name	avanto (462), sonata (160), trio (52), triotim (582),
Sequence name	*tfl3d1 (13), *tfl3d1_ns (983), spc3d1rr282ns (5), tfl3d1 (1), tfl3d1_ns (254),
Repetition time	1660 (3), 1960 (13), 2250 (539), 2300 (615), 2730 (81), 3200 (5),
Echo time	2.02 (3), 2.86 (1), 2.92 (22), 2.94 (1), 2.95 (462), 2.96 (183), 2.99 (14), 3.03 (348), 3.04 (1), 3.08 (1), 3.11 (1), 3.13 (1), 3.55 (1), 3.68 (148), 3.93 (51), 4.43 (7), 4.58 (3), 401 (5), 5.59 (3),
Inversion time	1000 (81), 1100 (627), 750 (3), 850 (539), 900 (1), null (5),
Magnetic field strength	1.494 (101), 1.5 (521), 2.89362 (52), 3 (582),
Number of phase encoding steps	176 (3), 196 (5), 253 (5), 255 (565), 256 (677), 320 (1),
Pixel bandwidth	130 (636), 140 (611), 240 (1), 260 (3), 751 (5),
Transmitting coil	body (1068), cp_head (49), txrx_head (139),
Flip angle	120 (5), 15 (539), 7 (81), 8 (630), 9 (1),
Tcoil ID/receiving coil	32ch_head (215), 8ch_head (573), body (1), cp_headarray (256), headmatrix (70), null (2), txrx_head (139),

Each scanning setting is followed by the number of subjects that have been scanned using this setting.

the method still allows for other genetic variants to be revealed as well.

MATERIALS AND METHODS

Participants

BIG

A large cohort was used for discovery to increase the statistical power. This step was performed using the Brain Imaging Genetics (BIG) dataset, an ongoing effort being conducted at the Radboud University Nijmegen together with the Max Planck Institute for Psycholinguistics (Nijmegen, the Netherlands) [Bralten et al., 2011; Cousijn et al., 2012]. The regional medical ethics committee approved the study and all subjects provided written informed consent. Specifically in this work, a total of 1,256 healthy Caucasians were admitted into the investigation, including 617 males (age: 23.28 ± 4.11 years) and 843 females (age: 22.67 ± 3.61 years) for which both neuroimaging and genotype data were collected [Guadalupe et al., 2014]. All subjects are typically highly educated and free of neurological or psychiatric history according to self-report. To be noted, an overlap of subjects might exist between the present study and Chavarria-Siles et al.'s study. The latter employed 532 healthy BIG subjects.

MCIC

In the validation step, we used the subjects from the Mind Clinical Imaging Consortium (MCIC) study [Gollub et al., 2013], a collaborative effort of four research teams from University of New Mexico-Mind Research Network, Massachusetts General Hospital, University of Minnesota, and University of Iowa. The institutional review board at each site approved the study and all subjects provided written informed consent. Out of 255 subjects, 89 were healthy Caucasians, including 51 males (age: 31.41 ± 10.39 years) and 38 females (age: 33.61 ± 11.50 years). These subjects were employed to validate the results obtained from the BIG data. All healthy subjects were screened to ensure that they were free of any medical, neurological, or psychiatric illnesses, including any history of substance abuse.

Neuroimaging

BIG

Structural images were acquired at the Donders Centre for Cognitive Neuroimaging (Nijmegen, The Netherlands) using different scanners, i.e., 1.5 T Siemens Avanto and Sonata, as well as 3.0 T Siemens Trio and TIM Trio. Transmitting and receiving coils also differed across subjects. A standard sagittal T_1-weighted three-dimensional magnetization prepared rapid gradient echo (MP-RAGE) sequence was employed, while some variations were observed in repetition, inversion, and echo time, as well as pixel bandwidth and flip angle. The use of parallel imaging with an acceleration factor of 2 was also included. Table I summarizes the settings used in BIG sMRI scans.

MCIC

The MCIC structural images were coronal T_1-weighted MRIs collected at multiple sites. Table II lists the setting used in the scans. It can be seen that scanners differed among 1.5 T Siemens Sonata and GE Signa, as well as 3.0 T Siemens Trio. Closely matched acquisition sequences were used. However, repetition time and pulse sequence varied somewhat.

Preprocessing

The T_1-weighted sMRI data were preprocessed at the Mind Research Network with Statistical Parametric Mapping 5 (SPM5, http://www.fil.ion.ucl.ac.uk/spm) using unified segmentation [Ashburner and Friston, 2005] in which image registration, bias correction, and tissue classification are performed using a single integrated algorithm.

TABLE II. Summary of MCIC scanning parameters

Site	M021 (51)	M552 (92)	M554 (47)	M871 (44)
Scanner	Siemens Avanto	GE Signa	Siemens Trio	Siemens Sonata
Scanning sequence	GR	RM	IR\GR	GR
Sequence name	*fl3d1_ns	N/A	*tfl3d1_ns (19), tfl3d1_ns (28)	*fl3d1_ns (35), fl3d1_ns (9)
Slice thickness (mm)	1.5	1.5 (20), 1.6 (38), 1.7 (31), 1.8 (3)	1.5	1.5
TR/TE (ms)	12/4.76	20/6	2530/3.81	12/4.76
Number of averages	1	1 (2), 2 (90)	1	1
Magnetic field strength (T)	1.494	1.5	2.8936	1.494
Number of phase encoding steps	256	N/A	256	288
Percent phase field of view	100	100	100	100
Pixel bandwidth	160	122	180	110
Receiving coil	cp_head	8ch_head	8ch_head	8ch_head
Acquisition matrix	0 256 256 0	0 256 256 0	0 256 256 0	0 256 256 0
Flip angle	20	30	7	20
Pixel spacing	0.625 0.625 (11), 0.70313 0.70313 (40)	0.625 0.625 (32), 0.66406 0.66406 (16), 0.70313 0.70313 (44)	0.625 0.625	0.625 0.625 (42), 0.70313 0.70313 (2)

Each site is followed by the number of subjects that have been scanned using this setting, which also applies if a scanning setting varies within a site.

In this way, brains were segmented into gray matter, white matter, and cerebrospinal fluid and nonlinearly transformed into the ICBM152 standard space without Jacobian modulation. The resulting GMD images were re-sliced to $2 \times 2 \times 2$ mm, resulting in $91 \times 109 \times 91$ voxels. In the subsequent quality check, we excluded outliers whose correlations between the individual images and the across-subject average image were 4 standard deviations less than the mean. Based on this criterion, four subjects were excluded from the BIG data and no outliers were identified for the MCIC data. A mask was then generated (mean GMD > 0) to include only the segmented gray matter voxels, resulting in a total of 298,707 voxels for the BIG data and 292,998 voxels for the MCIC data. A voxelwise linear regression was performed to remove age and sex effects to avoid capturing associations majorly driven by these factors in the subsequent analysis. Furthermore, considering that the images were acquired with various scanning platforms, we employed the source-based-morphometry (SBM) approach [Xu et al., 2009] to investigate and eliminate the image variability introduced by scanning settings [Chen et al., 2014b]. Specifically, the data were decomposed into a linear combination of underlying sources using independent component analysis (ICA) [Amari, 1998; Bell and Sejnowski, 1995]. The loadings of each component were then assessed for associations with available scanning parameters. Components significantly affected by scanning settings were then identified and eliminated from the original data. Following this, nine scanning-related components were removed for the BIG data (Table I) and eight scanning-related components removed for the MCIC data (Table II). After correction, we did not observe any significant scanning effects. Finally, the corrected data were smoothed with an 8-mm full width at half-maximum Gaussian kernel and thresholded at mean GMD > 0.1 (resulting in 274,131 voxels) for the subsequent association analysis.

Genotyping

BIG

Saliva samples were collected from participants for DNA extraction. Genotyping was then conducted using the Affymetrix GeneChip SNP 6.0 array spanning more than 906,600 SNPs. The call rate threshold was set to 90%.

MCIC

DNA was extracted from blood samples. Genotyping for all participants was performed using the Illumina Infinium HumanOmni1-Quad assay spanning 1,140,419 SNP loci. BeadStudio was used to make the final genotype calls.

Imputation

To maximize the number of overlapping SNPs between two datasets, we imputed the MCIC data up to 5M SNPs using the MACH/Minimac pipeline [Howie et al., 2012] leveraging a large reference panel of the 1,000 Genomes data [Altshuler et al., 2012], as described in the ENIGMA protocol (http://enigma.ini.usc.edu/). We further excluded those imputed SNPs whose estimates of the squared correlations between imputed genotypes and true

unobserved genotypes (rsq) were lower than 0.3, as recommended by the developer of the tool. To be consistent with the BIG data, the MCIC genotype data were obtained based on the continuous imputation data using the Genome-wide Complex Trait Analysis (GCTA) tool [Yang et al., 2011].

Data cleaning

PLINK software [Purcell et al., 2007] was used to perform a series of standard quality control procedures. SNPs and subjects were first examined for a genotyping rate threshold of 90%; SNPs were excluded if they showed deviation from Hardy–Weinberg Equilibrium with a threshold of 10^{-6} or if they failed to be missing at random with a threshold of 10^{-10}; minor allele frequency cut-off was set to 0.01. Potential relatives were excluded if the Identity-By-Descent (IBD) was higher than 0.1875. For the BIG data, we first replaced the missing genotypes using haplotype genotypes of high linkage disequilibrium (LD) loci (correlation >0.85). After the above procedures, missing genotypes were still observed in 134,607 out of 671,782 autosomal SNPs with missing ratios no greater than 0.05. We then replaced the remaining missing genotypes using the major alleles of individual loci. Discrete numbers were then assigned to the categorical genotypes: 0 for no minor allele, 1 for one minor allele, and 2 for two minor alleles. Finally, 666,019 common loci were genotyped or imputed in both the BIG and MCIC data. These loci were included for the association and validation analysis.

Association Analysis

pICA-R [Chen et al., 2013] was employed to identify relationships between hidden factors of particular attribute within two data modalities, as illustrated in Figure 1. In this work, pICA-R estimates underlying components for the GMD images (Modality 1) and the SNP data (Modality 2) independently and in parallel. The data decomposition builds upon the regular infomax ICA framework [Bell and Sejnowski, 1995], which identifies sets of co-varying variables that are independent from each other and organizes them into different components, as described in Eq. (1), where **X** represents the observed data matrix (subject × voxel/SNP); **S, A,** and **W** denote the component, loading/mixing, and unmixing matrix, respectively. The subscript d runs from 1 to 2, denoting the data modality.

$$X_d = A_d S_d \rightarrow S_d = W_d X_d,\ A_d = W_d^{-1},\ d = 1,2$$
$$Y_d = \frac{1}{1+e^{-U_d}},\ U_d = W_d X_d + W_{d0} \tag{1}$$

Mathematically, pICA-R iteratively updates the unmixing matrices $\mathbf{W_1}$ and $\mathbf{W_2}$ to gradually optimize the objective functions F_1, F_2, and F_3, as described in Eqs. (2) and (3). F_1 is the objective function of the regular infomax for Modality 1, where independence among components is achieved by maximizing the entropy H. $f_y(Y)$ is the probability density function of the sigmoid function Y. E is the expected value and $\mathbf{W_0}$ is the bias vector. In contrast, F_2 is the objective function for Modality 2, where an additional Euclidean distance metric is imposed to extract maximally independent components, one of which also closely resembles the reference **r**. To avoid false positives, the constraint weight λ is adaptively adjusted so that the distance metric is not over-emphasized. The inter-modality correlation function F_3 is designed to maximize the correlations computed over the columns of the loading matrices $\mathbf{A_1}$ and $\mathbf{A_2}$, capturing connections between pairs of inter-modality components.

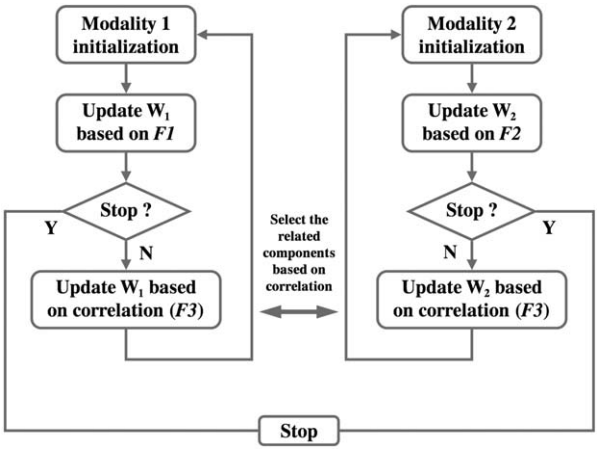

Figure 1.

Flow chart of pICA-R. $\mathbf{W}_1$ and $\mathbf{W}_2$ denote the unmixing matrices of the two modalities, respectively. F_1, F_2, and F_3 represent the objective functions based on which unmixing matrices are updated.

$$\begin{aligned} F_1 &= \max\{H(Y_1)\} = \max\left\{-E\left[\ln f_{y1}(Y_1)\right]\right\} \\ F_2 &= \max\left\{\lambda H(Y_2) + (1-\lambda)\left[-\mathrm{dist}^2\left(\tilde{r}, |\tilde{S}_{2k}|\right)\right]\right\} \\ &= \max\left\{\lambda\left(-E\left[\ln f_{y2}(Y_2)\right]\right) + (1-\lambda)\left(-\left|\left|\left|W_{2k}\tilde{X}_2\right| - \tilde{r}\right|\right|_2^2\right)\right\} \end{aligned} \tag{2}$$

$$F_3 = \max\left\{\sum_{i,j}\mathrm{Corr}^2(A_{1i}, A_{2i})\right\} = \max\left\{\sum_{i,j}\frac{\mathrm{Cov}^2(A_{1i}, A_{2i})}{\mathrm{Var}(A_{1i})\mathrm{Var}(A_{2i})}\right\} \tag{3}$$

The reference **r** is a binary vector with the same number of loci as the genomic data, where the selected referential loci are set to "1" and the rest are "0"s. This binary reference serves as a mask such that the distance between the component and reference vector is optimized particularly for the referential loci only. This design enables a semi-blind decomposition, where the presumed causal loci are constrained to be highlighted in the resulting component while the remaining loci are allowed to show their own

importance driven by the data. For a full description of the mathematical details of pICA-R, we refer readers to the original publication [Chen et al., 2013].

Specifically in this work, the genetic references were derived from genes encoding heterotrimeric G-proteins. We leveraged the results from an imaging genetics study reporting associations between gray matter volume variations and SNPs in G-protein coding genes [Chavarria-Siles et al., 2013]. Among the seven genes identified in that previous work, *GNA15*, *GNAO1*, and *GNB5* covered less than 10 SNPs in our data, therefore were not tested as references given that simulation results suggested an optimal reference of 20 true causal loci [Chen et al., 2013]. For the remaining four genes, *GNG2*, *GNAQ*, *GNA14*, and *GNAL*, we identified the corresponding SNPs in each gene and grouped neighboring SNPs with moderate correlations ($r^2 > 0.2$, [Ripke et al., 2011]) into a cluster. The largest cluster within each gene was then used as the reference. This is because SNPs in one gene do not necessarily contribute simultaneously to only a single component, which is against the design of pICA-R. Instead, SNPs in one LD cluster are more likely to contribute to the same component and serve as good candidates for reference given that a marker allele in LD with the causal variant should show (by proxy) an association with the trait of interest [Stranger et al., 2011]. In this way, we tested four references hosted by *GNG2*, *GNAQ*, *GNA14*, and *GNAL*.

Like infomax ICA, pICA-R requires estimating the number of components before data decomposition. Minimum description length (MDL) [Rissanen, 1978] is commonly used for the imaging modality to select the component number yielding the most efficient representation of the original data. However in the SNP data, most genetic factors account for small amounts of variance, except for those related to population structure. Thus, MDL is much less applicable to select the component number such that the major variance in the data is retained. Instead, we chose to estimate the component number based on components' consistency, to obtain the most stable data decomposition [Chen et al., 2012].

Validation

The genetic references were implicated in the work by Chavarria-Siles et al. [2013] which used a portion of the current BIG data. Unfortunately, we did not have a detailed list of the subjects used in that work and could not investigate whether our finding would hold in the non-overlapping portion of the BIG data. Instead, we used the independent MCIC data to assess the validity of the imaging genetic associations identified in the BIG data. As pICA-R's performance would significantly degrade given the MCIC sample size of 89 and 666,019 SNPs [Chen et al., 2013], we chose to project the sMRI and SNP components identified in the BIG data to the MCIC data to obtain the new loading coefficients, as described in Eq. (4):

$$\begin{aligned} \tilde{S}_d^{\mathrm{BIG}^{-1}} &= S_d^{\mathrm{BIG}^{-1}}|_{\text{top voxels /SNPs,}}\ d=1,2 \\ A_d^{\mathrm{MCIC}} &= \tilde{X}_d^{\mathrm{MCIC}}\ \tilde{S}_d^{\mathrm{BIG}^{-1}} \end{aligned} \tag{4}$$

where the subscript "d" runs from 1 to 2, denoting the sMRI and SNP modality, respectively. $\mathbf{S_d^{BIG^{-1}}}$ represents the pseudo inverse of the component matrix extracted from the BIG data. $\tilde{\mathbf{S}}_\mathbf{d}^{\mathbf{BIG^{-1}}}$ and $\tilde{\mathbf{X}}^{\mathbf{MCIC}}$ denote respectively the submatrices of $\mathbf{S^{BIG^{-1}}}$ and the MCIC observed data, corresponding to the top voxels or SNPs presenting relatively stronger correlations with the loadings. $\mathbf{A^{MCIC}}$ represents the loaing matrix estimated through projecting the top voxels or SNPs. We expect that the loadings obtained in this way should more accurately reflect the effects of the most important markers. Finally, the correlations between the projected loadings were calculated to assess whether the sMRI-SNP association identified in the BIG data remained significant in the MCIC data.

Analyzing Components

To understand the influences on cognition, the identified SNP and sMRI components were further investigated for associations with available phenotypic data, which was the reversal learning score collected for 599 out of 1,256 BIG subjects. In addition, top contributing voxels of the identified sMRI component were mapped to the Talairach atlas [Lancaster et al., 1997, 2000] for the involved brain regions. Meanwhile, top contributing SNPs were annotated and the hosting genes were sent for Ingenuity Pathway analysis (IPA, http://www.ingenuity.com/) to reveal the genetic architecture.

RESULTS

The number of components was estimated to be 10 and 11 for the sMRI and SNP data, respectively. Among all the tested references, the one derived from *GNA14* elicited a significant sMRI-SNP association ($r = -0.16$, $P = 2.27 \times 10^{-8}$). This exceeded the conservative Bonferroni threshold of 1.14×10^{-4} which corrected for all the tested four genetic references and the combinations of all extracted components (10 sMRI $\times$ 11 SNP) in each run. The reference comprised 22 out of 83 SNPs from *GNA14*, as listed in Supporting Information Table S1. These SNPs are in moderate LD, presenting a mean r-square of 0.54, and distanced by an average of 2,557 base pairs. The sMRI-SNP association remained significant, exhibiting a correlation of -0.16 ($P = 2.34 \times 10^{-8}$) when the SNP component was controlled for age and sex, as shown in Figure 2a. Besides, the SNP-sMRI association remained significant ($P = 3.30 \times 10^{-7}$) when the top three principal components of the SNP data were further included as covariates [Ripke et al., 2011], indicating that the observed association was not likely attributable to ancestral background. The associated

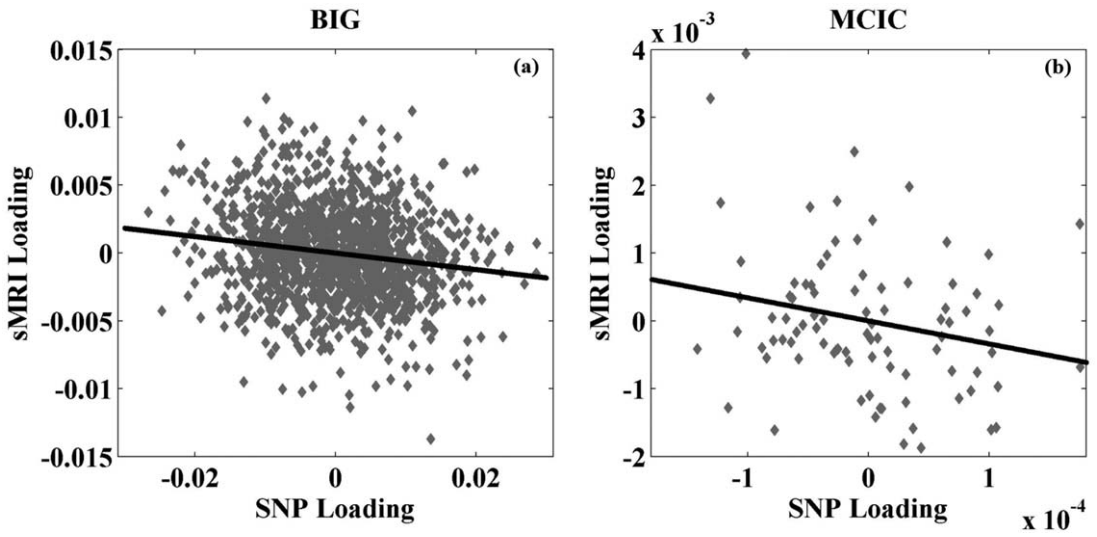

Figure 2.
Scatter plots of (**a**) the single nucleotide polymorphism (SNP) and sMRI loadings identified in the BIG data; and (**b**) the SNP and sMRI loadings obtained from the MCIC data through projection.

sMRI component was thresholded at $|Z| > 2$ for top voxels. The number of top SNPs was determined based on the absolute values of the component z-scores using a more conservative linear fitting approach (for details see Supporting Information Figure S1), yielding a total of 2,000 top SNPs corresponding to $|Z| > 3.37$. We then projected the top voxels and SNPs to the MCIC data, and the resulting loadings again yielded a significant correlation of -0.25 ($P = 0.02$) when controlling for age and sex, as shown in Figure 2b. To be noted, the projected association was robust to the threshold selection, remaining significant with a number of top SNPs ranging from 1,000 to 2,500. No association was observed between the identified sMRI/SNP component and the reversal learning score.

The top contributing voxels of the sMRI component were further mapped to nearest gray matter to obtain the Talairach atlas labels [Lancaster et al., 1997, 2000]. Figure 3 and Table III show the spatial map and the mapped regions, respectively. It can be seen that the identified brain network comprised superior and medial frontal gyri, precuneus, and cingulate gyrus. For the SNP component, Supporting Information Table S2 provides a summary of

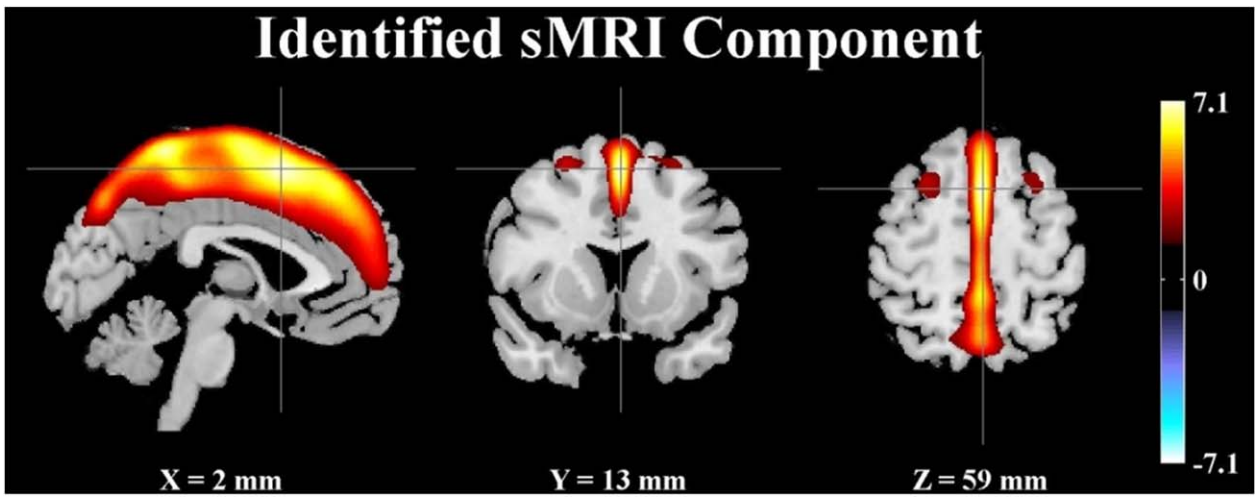

Figure 3.
Spatial map of the identified sMRI component ($|Z| > 2$). [Color figure can be viewed in the online issue, which is available at wileyonlinelibrary.com.]

TABLE III. Talairach labels of identified brain regions (|Z| > 2)

Brain region	Brodmann area	L/R volume (cm^3)	L/R random effects, max Z (*x*, *y*, *z*)
Medial frontal gyrus	6, 8, 32, 9, 10	13.9/8.7	6.53 (0,16,47)/5.79 (2,−6,65)
Superior frontal gyrus	6, 8, 9, 10	12.3/9.6	7.15 (0,14,53)/6.01 (2,14,53)
Precuneus	7, 19	8.0/6.0	6.44 (0,−47,63)/6.29 (2,−47,63)
Paracentral lobule	5, 4, 6, 31, 7	5.2/4.1	7.01 (0,−41,65)/6.63 (2,−43,63)
Cingulate gyrus	24, 32, 31	4.0/2.0	5.59 (0,2,48)/4.79 (2,18,43)
Postcentral gyrus	5, 7, 4, 3, 2	3.5/3.5	6.75 (−2,−41,65)/6.81 (2,−41,65)
Middle frontal gyrus	6, 8	2.7/2.9	2.88 (−28,1,61)/3.38 (28,5,59)

the top contributing SNPs, including chromosome, base pair position, corresponding gene, minor allele, and component *z*-score. From the *GNA14* reference, five SNPs were identified as top contributors to the associated SNP component, including rs10869927_G ("G" for the minor allele), rs10781441_T, rs12684903_A, rs2889774_T, and rs7047853_G. Figure 4 shows a Manhattan plot of weights of loci for the identified SNP component, where clusters are marked if they span more than five SNPs with maximum normalized weights greater than 5. Out of the top 2,000 SNPs, 803 are intragenic and mapped to 272 unique genes, including another G-protein, *GNA12*, and two G-protein-coupled receptors, *GPR113* and *GPR133*. IPA revealed that these 272 genes were significantly enriched in a number of canonical pathways, including synaptic long-term potentiation (LTP) and depression (LTD), axonal guidance, protein kinase A (PKA), CREB, and nNOS signaling, as listed in Table IV. In particular, all the pathways highlighted in bold remained significantly enriched when the number of top SNPs was adjusted from 1,000 to 2,500, indicating a relatively consistent genetic architecture. We also explored through IPA potential interactions between selected genes of interest, including *GNA12*, *GNA14*, *GRM1*, *PRKCD*, *CAMK2B*, and *PDIA3*. The constructed network is illustrated in Supporting Information Figure S2.

DISCUSSION

In this work, we applied pICA-R to explore genomic basis of brain structure in a homogeneous cohort of healthy Caucasians. G-proteins arose as potential references given that they are implicated in neural development. A previous univariate study [Chavarria-Siles et al., 2013] provided more direct evidence for associations between G-protein SNPs and regional gray matter variations. We then leveraged these results and derived four genetic references which were then investigated in the semi-blind multivariate framework. In the BIG dataset which included 1,256 subjects, a *GNA14* reference elicited a significant SNP-sMRI association ($r = -0.16$, $P = 2.34 \times 10^{-8}$), while the other three tested references did not yield any significant finding. As discussed by Chen et al. [2013], references derived from univariate models do not always yield significant findings in multivariate analyses. This might be due to various factors. One possibility is that the reference SNPs may have heterogeneous effects and contribute to different components. Or the related network as a whole may not be well represented in this specific dataset.

Using a semi-blind multivariate approach, we identified extended SNP and sMRI components compared to the previous work by Chavarria-Siles et al. The identified brain network consisted of medial frontal gyrus, superior frontal gyrus, precuneus, and cingulate regions. To be noted, the medial frontal cortex was also identified by the Chavarria-Siles et al. that employed 532 BIG subjects and used a different method. Regarding the genetic modality, five reference SNPs from *GNA14*, as expected, were identified as top contributors to the associated SNP component. The SNP highlighted in Chavarria-Siles et al. (rs4745639) was not included in the reference, however it showed moderate LD with rs2889774 and rs10869927 (r^2 of 0.15 and 0.14, respectively), and all contributed with negative component weights. The elicited SNP component was enriched in pathways related to neuronal functions, as listed in Table IV. More importantly, the identified association was further replicated in the independent MCIC dataset. Compared to univariate analyses, pICA-R assesses multiple

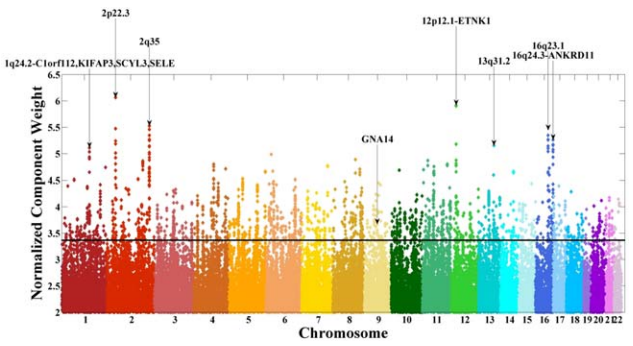

Figure 4.

Manhattan plot for the identified single nucleotide polymorphism (SNP) component. The horizontal line indicates the threshold at |Z| > 3.37 for selection of top contributing SNPs. Clusters are marked if they span more than 5 SNPs with maximum normalized weights greater than 5. The GNA14 cluster is also marked. [Color figure can be viewed in the online issue, which is available at wileyonlinelibrary.com.]

TABLE IV. Pathway analysis on the identified SNP component

Ingenuity canonical pathways	Molecules	*P*-value
Neuropathic pain signaling in dorsal horn neurons	NTRK2, KCNQ2, GRM1, PDIA3, KCNQ3, PRKCH, CAMK2B	6.76 *E*−04
Inositol pyrophosphates biosynthesis	IP6K3, PPIP5K1	4.37 *E*−03
Histidine degradation III	UROC1, AMDHD1	5.75 *E*−03
Histidine degradation VI	UROC1, AMDHD1	7.41 *E*−03
Synaptic long-term potentiation	**GRM1, PDIA3, PRKCH, GNA14, ADCY8, CAMK2B**	**7.59 *E*−03**
Protein kinase A signaling	**EPM2A, PTPRK, PTPRD, PTPRJ, PDIA3, PDE8B, PRKCH, ADCY8, EYA2, PTPRT, NTN1, CAMK2B**	**8.51 *E*−03**
Axonal guidance signaling	**PDIA3, GNA12, GNA14, ADAMTS2, NTN1, SRGAP3, NTRK2, NTRK3, EFNA5, PAK7, PRKCH, WNT5A, GLIS1**	**1.05 *E*−02**
CREB signaling in neurons	**GRM1, PDIA3, GNA12, PRKCH, GNA14, ADCY8, CAMK2B**	**1.32 *E*−02**
Synaptic long-term depression	**GRM1, PDIA3, GNA12, PLA2R1, PRKCH, GNA14**	**1.62 *E*−02**
Sulfate activation for sulfonation	PAPSS2	2.95 *E*−02
Formaldehyde oxidation II (glutathione-dependent)	ESD	2.95 *E*−02
Glutamine degradation I	GLS	2.95 *E*−02
nNOS signaling in neurons	**DLG2, PRKCH, NOS1AP**	**3.09 *E*−02**
Endothelin-1 signaling	PDIA3, GNA12, PLA2R1, PRKCH, GNA14, ADCY8	3.89 *E*−02
GNRH signaling	PAK7, PRKCH, GNA14, ADCY8, CAMK2B	4.07 *E*−02
RhoGDI signaling	GNA12, ARHGAP12, CDH18, PAK7, GNA14, CDH13	4.37 *E*−02
Methionine salvage II (Mammalian)	BHMT2	4.37 *E*−02

variables for the aggregate effect. For the SNP modality, pICA-R is well posed to model polygenicity and to capture the additive effect of multiple SNPs with moderate individual effects [Chen et al., 2013; Polderman et al., 2015]. For the sMRI modality, pICA-R extracts patterns of variations shared by regional and distant voxels [Xu et al., 2009]. And imaging genetic associations are then evaluated between the SNP and sMRI components' loadings. Thus, our results delineate a genomic basis underlying a proportion of the GMD variation in the highlighted frontal and parietal regions.

The spatial map of the identified sMRI component clearly highlighted the midline of brain, which is frequently implicated in neural development, ageing, and cognition [Frangou et al., 2004; Lyuksyutova et al., 2003; Shaw et al., 2006; Sowell et al., 2003]. Prefrontal cortex is known to be involved in complex cognitive behavior and decision making [Koechlin and Hyafil, 2007; Koechlin et al., 2003]. Precuneus plays a key role in highly integrated tasks, including episodic memory retrieval, self-referential processes, and consciousness [Laureys et al., 2004; Lundstrom et al., 2005; Ochsner et al., 2004]. Cingulate cortex is an integral part of the limbic system and active in a variety of cognitive functions such as emotion, learning and memory [Bush et al., 2000]. More interestingly, these regions are also among those showing relatively significant structural variations for different age and intelligence groups. A VBM study demonstrated positive correlations between IQ and GMD in voxel clusters distributed along the brain midline, including frontal cortex, cingulate, and precuneus [Frangou et al., 2004]. At superior and medial frontal gyri, the trajectories of cortical thickness change with age are found to be different between the superior and the high/average intelligence groups [Shaw et al., 2006]. Besides, axons extend on either side of the midline (anterior–posterior axis) to form longitudinal tracts and the midline cells are crucial for guiding axon outgrowth [Lyuksyutova et al., 2003]. These observations suggest that the identified brain network captures regional GMD covariations that can play a role in cognitive abilities and might reflect inter-individual differences in brain development.

The SNP component was overrepresented in a number of pathways communicating with each other and with G-proteins. From those shown in Table IV, LTP and LTD are two forms of synaptic plasticity that affect signal transmission between neurons and have been widely studied to understand the mechanisms underlying learning and memory [Martin et al., 2000; Neves et al., 2008]. It is believed that glutamate receptors are major triggers for the induction of LTP and LTD, where PKA, protein kinase C (PKC), calcium/calmodulin-dependent protein kinase II

(CaMKII) can all play a role [Collingridge et al., 2004]. CREB is majorly activated by cAMP through PKA [Delghandi et al., 2005]. In particular, a behavioral experience can elicit synaptic activities which activate CREB, inducing expression of molecules contributing to consolidating changes in synaptic strength [Benito and Barco, 2010]. Axon guidance strongly relies on a number of cue molecules, among which netrins are the most well understood. It has been demonstrated that netrins retain the function of attracting axons toward the brain midline while also repelling some axons, and responses to the guidance cue netrin-1 (*NTN1*) are sensitive to levels of cAMP or PKA activity [Dickson, 2002]. Neuronal nitric oxide synthase (nNOS) is a biosynthetic enzyme functioning in several types of synaptic plasticity, including LTP and LTD [Bon and Garthwaite, 2003; Nelson et al., 1995]. The phosphorylation of nNOS is regulated by kinases and phosphatases such as PKA, PKC, and CaMKII [Zhou and Zhu, 2009]. It is noteworthy that G-proteins are involved in the signaling cascades of all these cellular machineries, including glutamate, cAMP, PKA, PKC, CREB, and CaMKII [Neves et al., 2002].

Among the enriched pathways, overlaps of genes were observed, including *GRM1*, *PRKCH*, *GNA12*, *GNA14*, and *CAMK2B*. *GRM1* encodes a metabotropic, G protein-coupled receptor for glutamate, the major excitatory neurotransmitters in the central nervous system [Hermans and Challiss, 2001]. A total of 10 SNPs from *GRM1* were identified as top contributors to the component in our analysis. Nine out of these 10 SNPs contributed positively (see Supporting Information Table S2 for details). Note that the SNP-sMRI correlation was negative, indicating that subjects with higher loads of the SNP component carried relatively lower loads of the sMRI component. Also, the highlighted brain regions presented positive component weights, indicating that subjects with higher loads of the sMRI component had higher regional GMD. Thus, for these SNPs presenting positive component weights, our finding suggested that, overall, subjects carrying more minor alleles at these loci showed reduced GMD in the highlighted brain regions. Only one out of the 10 top SNPs in *GRM1* (rs854144_T) contributed with a negative weight, indicating more minor alleles found in subjects exhibiting increased regional GMD. *PRKCH* is another molecule of great importance as it encodes a PKC subtype. PKCs phosphorylate a wide range of protein targets involved in brain functioning. For instance, phosphorylation of *GluR1* by PKC is demonstrated to be critical for LTP expression [Boehm et al., 2006]. In our analysis, one single SNP rs1957902_G was identified from *PRKCH*, presenting a negative weight. *GNA12* and *GNA14* fall into the G-protein subfamilies of G_{12} and G_q. *GNA12* has been indicated to negatively regulate cell adhesion through interacting with cadherin [Meigs et al., 2002]. *GNA14* is among the genes which were found to exhibit developmental expression variations in the cortex of a marmoset animal model, and linked to axonal guidance [Sasaki et al., in press]. In the present study, rs2258960_T and rs2644311_T were identified from *GNA12* and presented positive weights. For *GNA14*, rs10869927_G and rs2889774_T showed negative weights while rs10781441_T, rs12684903_A, and rs7047853_G showed positive weights. *CAMK2B* encodes a Ca^{2+}/calmodulin-dependent protein kinase involved in calcium signaling. The expression of this gene has been found to be disrupted in Alzheimer's disease [Antonell et al., 2013; Liang et al., 2008]. Three SNPs, rs12702075_A, rs10281178_C, and rs3934888_G, were identified from *CAMK2B*, all exhibiting negative weights.

Both the imaging and genetic findings from our analysis link strongly to neural development, indicating that the observed GMD variations might be traced back to developmental processes under control of genetic factors. It is well acknowledged that genetic components underlie anatomic variations in healthy and diseased human brains [Andersen, 2003; Giedd, 2005; Sotelo, 2004]. Direct associations between genetic variants and quantitative structural measures have also been demonstrated in large-scale studies [Bis et al., 2012; Stein et al., 2012]. Compared with previous works using univariate approaches, our results delineate relationships between particular genetic pathways and regional structural variations, emphasizing that these G-protein-related PKA, CREB, and nNOS mechanisms play a critical role in brain development which might ultimately lead to GMD differences. On the other hand, it should be noted that brain structure is the final manifestation of a complex interplay between multiple genetic and environmental factors. Our analysis captured a part of the story.

The current study benefited from a large homogeneous discovery sample which enhances statistical power. In addition, the employed multivariate approach assessed a group of variables whose aggregate effects would be more prominent compared to those of individual variables. Leveraging prior knowledge further improved the chance of pinpointing factors of interest in a large complex dataset. Most importantly, the imaging genetic association identified from the discovery sample was replicated in an independent cohort, indicating a low possibility of false positive results. On the other hand, one major limitation of this study lies in the different scanning platforms employed for imaging data collection, which can be a potential confound. To address this issue, we carefully explored all the scanning settings and eliminated from the imaging data the variance most likely induced by scanning discrepancies based on a linear model. Nonlinear scanning effects might still exist for which we do not have any knowledge at present. However, such effects were not expected to significantly contribute to the identified imaging genetic association given the linear decomposition of ICA. Another limitation is that it is not clear yet how the identified components are related to behavior based on the available data. The identified local GMD variations have

been implicated in intelligence studies; however we did not collect IQ data in this project. Instead we investigated whether this imaging trait was correlated with the available reversal learning scores and found no significant associations. Further work needs to be done to better understand how the genetic and GMD variations might lead to differences in behavior. Besides, it should be noted that SNPs in high LD would exhibit comparable effects in our analysis. Therefore, SNPs might be identified due to tagging true causal variants. However, the identified genes and pathways should be unchanged. Finally, following the design of pICA-R, we only tested the largest cluster as a genetic reference for each candidate gene in this work, ignoring other smaller clusters which might also be biologically informative. This could be tackled with an extended approach, parallel ICA with multiple references [Chen et al., 2014a], which explores potential convergence of functional influences among genes. We plan to conduct such an analysis in a future study.

In summary, we performed a guided exploration in the present study, where a reference derived from the *GNA14* gene managed to elicit a genetic component significantly associated with an sMRI component in a semi-blind multivariate analysis. The associated genetic component highlighted several neural signaling pathways which appear to interact with each other and are active in synaptic plasticity and axonal guidance. Meanwhile, the identified brain network comprised regions recruited in various cognitive processes and robustly implicated in brain maturation and intelligence. Collectively, our study suggests a key role of G-proteins in the genetic architecture underlying normal GMD variations in frontal and parietal regions. We speculate that the observed GMD variations partially result from differential genetic modulation of brain development, though future longitudinal studies are needed to dissect genetic contribution to trajectories of anatomic changes in developing brains.

ACKNOWLEDGMENTS

This work makes use of the BIG (Brain Imaging Genetics) database, first established in Nijmegen, The Netherlands, in 2007. This resource is now part of Cognomics (www.cognomics.nl), a joint initiative by researchers of the Donders Centre for Cognitive Neuroimaging, the Human Genetics and Cognitive Neuroscience departments of the Radboud University Nijmegen Medical Centre and the Max Planck Institute for Psycholinguistics in Nijmegen. The Cognomics Initiative is supported by the participating departments and centres and by external grants, i.e. the Biobanking and Biomolecular Resources Research Infrastructure (Netherlands) (BBMRI-NL), the Hersenstichting Nederland, and the Netherlands Organisation for Scientific Research (NWO). The authors thank all persons who kindly participated in the BIG research. The Board of the Cognomics Initiative consists of Barbara Franke, Simon Fisher, Guillén Fernandez, Peter Hagoort, Han G. Brunner, Jan Buitelaar, Hans van Bokhoven and David Norris. The authors would also like to thank the University of Iowa Hospital, Massachusetts General Hospital, the University of Minnesota, the University of New Mexico, and the Mind Research Network staff for their efforts in data collection, preprocessing, and analyses.

REFERENCES

Altshuler DM, Durbin RM, Abecasis GR, Bentley DR, Chakravarti A, Clark AG, Donnelly P, Eichler EE, Flicek P, Gabriel SB, Gibbs RA, Green ED, Hurles ME, Knoppers BM, Korbel JO, Lander ES, Lee C, Lehrach H, Mardis ER, Marth GT, McVean GA, Nickerson DA, Schmidt JP, Sherry ST, Wang J, Wilson RK, Gibbs RA, Dinh H, Kovar C, Lee S, Lewis L, Muzny D, Reid J, Wang M, Wang J, Fang XD, Guo XS, Jian M, Jiang H, Jin X, Li GQ, Li JX, Li YR, Li Z, Liu X, Lu Y, Ma XD, Su Z, Tai SS, Tang MF, Wang B, Wang GB, Wu HL, Wu RH, Yin Y, Zhang WW, Zhao J, Zhao MR, Zheng XL, Zhou Y, Lander ES, Altshuler DM, Gabriel SB, Gupta N, Flicek P, Clarke L, Leinonen R, Smith RE, Zheng-Bradley X, Bentley DR, Grocock R, Humphray S, James T, Kingsbury Z, Lehrach H, Sudbrak R, Albrecht MW, Amstislavskiy VS, Borodina TA, Lienhard M, Mertes F, Sultan M, Timmermann B, Yaspo ML, Sherry ST, McVean GA, Mardis ER, Wilson RK, Fulton L, Fulton R, Weinstock GM, Durbin RM, Balasubramaniam S, Burton J, Danecek P, Keane TM, Kolb-Kokocinski A, McCarthy S, Stalker J, Quail M, Schmidt JP, Davies CJ, Gollub J, Webster T, Wong B, Zhan YP, Auton A, Gibbs RA, Yu F, Bainbridge M, Challis D, Evani US, Lu J, Muzny D, Nagaswamy U, Reid J, Sabo A, Wang Y, Yu J, Wang J, Coin LJM, Fang L, Guo XS, Jin X, Li GQ, Li QB, Li YR, Li ZY, Lin HX, Liu BH, Luo RB, Qin N, Shao HJ, Wang BQ, Xie YL, Ye C, Yu C, Zhang F, Zheng HC, Zhu HM, Marth GT, Garrison EP, Kural D, Lee WP, Leong WF, Ward AN, Wu JT, Zhang MY, Lee C, Griffin L, Hsieh CH, Mills RE, Shi XH, von Grotthuss M, Zhang CS, Daly MJ, DePristo MA, Altshuler DM, Banks E, Bhatia G, Carneiro MO, del Angel G, Gabriel SB, Genovese G, Gupta N, Handsaker RE, Hartl C, Lander ES, McCarroll SA, Nemesh JC, Poplin RE, Schaffner SF, Shakir K, Yoon SC, Lihm J, Makarov V, Jin HJ, Kim W, Kim KC, Korbel JO, Rausch T, Flicek P, Beal K, Clarke L, Cunningham F, Herrero J, McLaren WM, Ritchie GRS, Smith RE, Zheng-Bradley X, Clark AG, Gottipati S, Keinan A, Rodriguez-Flores JL, Sabeti PC, Grossman SR, Tabrizi S, Tariyal R, Cooper DN, Ball EV, Stenson PD, Bentley DR, Barnes B, Bauer M, Cheetham RK, Cox T, Eberle M, Humphray S, Kahn S, Murray L, Peden J, Shaw R, Ye K, Batzer MA, Konkel MK, Walker JA, MacArthur DG, Lek M, Sudbrak R, Amstislavskiy VS, Herwig R, Shriver MD, Bustamante CD, Byrnes JK, De la Vega FM, Gravel S, Kenny EE, Kidd JM, Lacroute P, Maples BK, Moreno-Estrada A, Zakharia F, Halperin E, Baran Y, Craig DW, Christoforides A, Homer N, Izatt T, Kurdoglu AA, Sinari SA, Squire K, Sherry ST, Xiao CL, Sebat J, Bafna V, Ye K, Burchard EG, Hernandez RD, Gignoux CR, Haussler D, Katzman SJ, Kent WJ, Howie B, Ruiz-Linares A, Dermitzakis ET, Lappalainen T, Devine SE, Liu XY, Maroo A, Tallon LJ, Rosenfeld JA, Michelson LP, Abecasis GR, Kang HM, Anderson P, Angius A, Bigham A, Blackwell T, Busonero F, Cucca F, Fuchsberger C, Jones C, Jun G, Li Y, Lyons R, Maschio A, Porcu E, Reinier F, Sanna S, Schlessinger D, Sidore C, Tan A, Trost MK, Awadalla P, Hodgkinson A, Lunter G, McVean GA, Marchini JL, Myers S,

Churchhouse C, Delaneau O, Gupta-Hinch A, Iqbal Z, Mathieson I, Rimmer A, Xifara DK, Oleksyk TK, Fu YX, Liu XM, Xiong MM, Jorde L, Witherspoon D, Xing JC, Eichler EE, Browning BL, Alkan C, Hajirasouliha I, Hormozdiari F, Ko A, Sudmant PH, Mardis ER, Chen K, Chinwalla A, Ding L, Dooling D, Koboldt DC, McLellan MD, Wallis JW, Wendl MC, Zhang QY, Durbin RM, Hurles ME, Tyler-Smith C, Albers CA, Ayub Q, Balasubramaniam S, Chen Y, Coffey AJ, Colonna V, Danecek P, Huang N, Jostins L, Keane TM, Li H, McCarthy S, Scally A, Stalker J, Walter K, Xue YL, Zhang YJ, Gerstein MB, Abyzov A, Balasubramanian S, Chen JM, Clarke D, Fu Y, Habegger L, Harmanci AO, Jin MK, Khurana E, Mu XJ, Sisu C, Li YR, Luo RB, Zhu HM, Lee C, Griffin L, Hsieh CH, Mills RE, Shi XH, von Grotthuss M, Zhang CS, Marth GT, Garrison EP, Kural D, Lee WP, Ward AN, Wu JT, Zhang MY, McCarroll SA, Altshuler DM, Banks E, del Angel G, Genovese G, Handsaker RE, Hartl C, Nemesh JC, Shakir K, Yoon SC, Lihm J, Makarov V, Degenhardt J, Flicek P, Clarke L, Smith RE, Zheng-Bradley X, Korbel JO, Rausch T, Stutz AM, Bentley DR, Barnes B, Cheetham RK, Eberle M, Humphray S, Kahn S, Murray L, Shaw R, Ye K, Batzer MA, Konkel MK, Walker JA, Lacroute P, Craig DW, Homer N, Church D, Xiao CL, Sebat J, Bafna V, Michaelson JJ, Ye K, Devine SE, Liu XY, Maroo A, Tallon LJ, Lunter G, McVean GA, Iqbal Z, Witherspoon D, Xing JC, Eichler EE, Alkan C, Hajirasouliha I, Hormozdiari F, Ko A, Sudmant PH, Chen K, Chinwalla A, Ding L, McLellan MD, Wallis JW, Hurles ME, Blackburne B, Li H, Lindsay SJ, Ning ZM, Scally A, Walter K, Zhang YJ, Gerstein MB, Abyzov A, Chen JM, Clarke D, Khurana E, Mu XJ, Sisu C, Gibbs RA, Yu FL, Bainbridge M, Challis D, Evani US, Kovar C, Lewis L, Lu J, Muzny D, Nagaswamy U, Reid J, Sabo A, Yu J, Guo XS, Li YR, Wu RH, Marth GT, Garrison EP, Leong WF, Ward AN, del Angel G, DePristo MA, Gabriel SB, Gupta N, Hartl C, Poplin RE, Clark AG, Rodriguez-Flores JL, Flicek P, Clarke L, Smith RE, Zheng-Bradley X, MacArthur DG, Bustamante CD, Gravel S, Craig DW, Christoforides A, Homer N, Izatt T, Sherry ST, Xiao CL, Dermitzakis ET, Abecasis GR, Kang HM, McVean GA, Mardis ER, Dooling D, Fulton L, Fulton R, Koboldt DC, Durbin RM, Balasubramaniam S, Keane TM, McCarthy S, Stalker J, Gerstein MB, Balasubramanian S, Habegger L, Garrison EP, Gibbs RA, Bainbridge M, Muzny D, Yu FL, Yu J, del Angel G, Handsaker RE, Makarov V, Rodriguez-Flores JL, Jin HJ, Kim W, Kim KC, Flicek P, Beal K, Clarke L, Cunningham F, Herrero J, McLaren WM, Ritchie GRS, Zheng-Bradley X, Tabrizi S, MacArthur DG, Lek M, Bustamante CD, la Vega D, Craig FM, Kurdoglu DW, Lappalainen AA, Rosenfeld T, Michelson JA, Awadalla LP, Hodgkinson P, McVean A, Chen GA, Tyler-Smith K, Chen C, Colonna Y, Frankish V, Harrow A, Xue J, Gerstein YL, Abyzov MB, Balasubramanian A, Chen S, Clarke JM, Fu D, Harmanci Y, Jin AO, Khurana MK, Mu E, Sisu XJ, Gibbs C, Fowler RA, Hale G, Kalra W, Kovar D, Muzny C, Reid D, Wang J, Guo J, Li X, Li G, Zheng Y, Altshuler X, Flicek DM, Clarke P, Barker L, Kelman J, Kulesha G, Leinonen E, McLaren R, Radhakrishnan WM, Roa R, Smirnov A, Smith D, Streeter RE, Toneva I, Vaughan I, Zheng-Bradley B, Bentley X, Cox DR, Humphray T, Kahn S, Sudbrak S, Albrecht R, Lienhard MW, Craig M, Izatt DW, Kurdoglu T, Sherry AA, Ananiev ST, Belaia V, Beloslyudtsev Z, Bouk D, Chen N, Church C, Cohen D, Cook R, Garner C, Hefferon J, Kimelman T, Liu M, Lopez C, Meric J, O'Sullivan P, Ostapchuk C, Phan Y, Ponomarov L, Schneider S, Shekhtman V, Sirotkin E, Slotta K, Xiao D, Zhang CL, Haussler H, Abecasis D, McVean GR, Alkan GA, Ko C, Dooling A, Durbin D, Balasubramaniam RM, Keane S, McCarthy TM, Stalker S, Chakravarti J, Knoppers A, Abecasis BM, Barnes GR, Beiswanger KC, Burchard C, Bustamante EG, Cai CD, Cao HY, Durbin HZ, Gharani RM, Gibbs N, Gignoux RA, Gravel CR, Henn S, Jones B, Jorde D, Kaye L, Keinan JS, Kent A, Kerasidou A, Li A, Mathias YR, McVean R, Moreno-Estrada GA, Ossorio A, Parker PN, Reich M, Rotimi D, Royal CN, Sandoval CD, Su K, Sudbrak YY, Tian R, Timmermann ZM, Tishkoff B, Toji S, Tyler-Smith LH, Via C, Wang M, Yang YH, Yang HM, Zhu L, Bodmer JY, Bedoya W, Ruiz-Linares G, Ming A, Yang CZ, You G, Peltonen CJ, Garcia-Montero L, Orfao A, Dutil A, Martinez-Cruzado J, Oleksyk JC, Brooks TK, Felsenfeld LD, McEwen AL, Clemm JE, Duncanson NC, Dunn A, Green M, Guyer ED, Peterson MS, Abecasis JL, Auton GR, Brooks A, DePristo LD, Durbin MA, Handsaker RM, Kang RE, Marth HM, McVean GT; Genomes project Consortium (2012): An integrated map of genetic variation from 1,092 human genomes. Nature 491:56–65.

Amari S (1998): Natural gradient works efficiently in learning. Neural Comput 10:251–276.

Andersen SL (2003): Trajectories of brain development: Point of vulnerability or window of opportunity? Neurosci Biobehav Rev 27:3–18.

Antonell A, Llado A, Altirriba J, Botta-Orfila T, Balasa M, Fernandez M, Ferrer I, Sanchez-Valle R, Molinuevo JL (2013): A preliminary study of the whole-genome expression profile of sporadic and monogenic early-onset Alzheimer's disease. Neurobiol Aging 34:1772–1778.

Ashburner J, Friston KJ (2005): Unified segmentation. Neuroimage 26:839–851.

Bell AJ, Sejnowski TJ (1995): An information-maximization approach to blind separation and blind deconvolution. Neural Comput 7:1129–1159.

Benito E, Barco A (2010): CREB's control of intrinsic and synaptic plasticity: Implications for CREB-dependent memory models. Trends Neurosci 33:230–240.

Bis JC, DeCarli C, Smith AV, van der Lijn F, Crivello F, Fornage M, Debette S, Shulman JM, Schmidt H, Srikanth V, Schuur M, Yu L, Choi SH, Sigurdsson S, Verhaaren BFJ, DeStefano AL, Lambert JC, Jack CR, Struchalin M, Stankovich J, Ibrahim-Verbaas CA, Fleischman D, Zijdenbos A, den Heijer T, Mazoyer B, Coker LH, Enzinger C, Danoy P, Amin N, Arfanakis K, van Buchem MA, de Bruijn RFAG Beiser A, Dufouil C, Huang JB, Cavalieri M, Thomson R, Niessen WJ, Chibnik LB, Gislason GK, Hofman A, Pikula A, Amouyel P, Freeman KB, Phan TG, Oostra BA, Stein JL, Medland SE, Vasquez AA, Hibar DP, Wright MJ, Franke B, Martin NG, Thompson PM, Nalls MA, Uitterlinden AG, Au R, Elbaz A, Beare RJ, van Swieten JC, Lopez OL, Harris TB, Chouraki V, Breteler MMB, De Jager PL, Becker JT, Vernooij MW, Knopman D, Fazekas F, Wolf PA, van der Lugt A, Gudnason V, Longstreth WT, Brown MA, Bennett DA, van Duijn CM, Mosley TH, Schmidt R, Tzourio C, Launer LJ, Ikram MA, Seshadri S; Cohorts for Heart and Ageing Research in Genomic Epidemiology Consortium (2012): Common variants at 12q14 and 12q24 are associated with hippocampal volume. Nat Genet 44:545–541.

Boehm J, Kang MG, Johnson RC, Esteban J, Huganir RL, Malinow R (2006): Synaptic incorporation of AMPA receptors during LTP is controlled by a PKC phosphorylation site on GluR1. Neuron 51:213–225.

Bon CLM, Garthwaite J (2003): On the role of nitric oxide in hippocampal long-term potentiation. J Neurosci 23:1941–1948.

Bralten J, Arias-Vasquez A, Makkinje R, Veltman JA, Brunner HG, Fernandez G, Rijpkema M, Franke B (2011): Association of the Alzheimer's gene SORL1 with hippocampal volume in young, healthy adults. Am J Psychiatry 168:1083–1089.

Bromberg KD, Iyengar R, He JC (2008): Regulation of neurite outgrowth by G(i/o) signaling pathways. Front Biosci 13:4544–4557.

Bush G, Luu P, Posner MI (2000): Cognitive and emotional influences in anterior cingulate cortex. Trends Cogn Sci 4:215–222.

Cabrera-Vera TM, Vanhauwe J, Thomas TO, Medkova M, Preininger A, Mazzoni MR, Hamm HE (2003): Insights into G protein structure, function, and regulation. Endocr Rev 24:765–781.

Chavarria-Siles I, Rijpkema M, Lips E, Arias-Vasquez A, Verhage M, Franke B, Fernandez G, Posthuma D (2013): Genes encoding heterotrimeric G-proteins are associated with gray matter volume variations in the medial frontal cortex. Cereb Cortex 23:1025–1030.

Chen J, Calhoun VD, Pearlson GD, Perrone-Bizzozero N, Sui J, Turner JA, Bustillo JR, Ehrlich S, Sponheim SR, Canive JM, Ho BC, Liu J (2013): Guided exploration of genomic risk for gray matter abnormalities in schizophrenia using parallel independent component analysis with reference. Neuroimage 83C:384–396.

Chen JY, Calhoun VD, Liu JY (2012): ICA order selection based on consistency: Application to genotype data. In: 2012 Annual International Conference of the Ieee Engineering in Medicine and Biology Society (Embc), San Diego, CA, USA, pp 360–363.

Chen J, Calhoun VD, Ulloa AE, Liu J (2014a): Parallel ICA with multiple references: A semi-blind multivariate approach. In: 2014 Annual International Conference of the IEEE Engineering in Medicine and Biology Society (Embc), Chicago, IL, USA, pp 6659–6662.

Chen J, Liu J, Calhoun VD, Arias-Vasquez A, Zwiers MP, Gupta CN, Franke B, Turner JA (2014b): Exploration of scanning effects in multi-site structural MRI studies. J Neurosci Methods C 230:37–50.

Collingridge GL, Isaac JTR, Wang YT (2004): Receptor trafficking and synaptic plasticity. Nat Rev Neurosci 5:952–962.

Cousijn H, Rijpkema M, Harteveld A, Harrison PJ, Fernandez G, Franke B, Arias-Vasquez A (2012): Schizophrenia risk gene ZNF804A does not influence macroscopic brain structure: An MRI study in 892 volunteers. Mol Psychiatry 17:1155–1157.

Delghandi MP, Johannessen M, Moens U (2005): The cAMP signalling pathway activates CREB through PKA, p38 and MSK1 in NIH 3T3 cells. Cell Signal 17:1343–1351.

Dickson BJ (2002): Molecular mechanisms of axon guidance. Science 298:1959–1964.

Ellison-Wright I, Glahn DC, Laird AR, Thelen SM, Bullmore E (2008): The anatomy of first-episode and chronic schizophrenia: An anatomical likelihood estimation meta-analysis. Am J Psychiatry 165:1015–1023.

Fischl B, Dale AM (2000): Measuring the thickness of the human cerebral cortex from magnetic resonance images. Proc Natl Acad Sci USA 97:11050–11055.

Frangou S, Chitins X, Williams SCR (2004): Mapping IQ and gray matter density in healthy young people. Neuroimage 23:800–805.

Frisoni GB, Fox NC, Jack CR, Scheltens P, Thompson PM (2010): The clinical use of structural MRI in Alzheimer disease. Nat Rev Neurol 6:67–77.

Giedd JN (2005): Trajectories of anatomic brain development in children and adolescents. Neuropsychopharmacology 30:S9–S9.

Giedd JN, Rapoport JL (2010): Structural MRI of pediatric brain development: What have we learned and where are we going? Neuron 67:728–734.

Gollub RL, Shoemaker JM, King MD, White T, Ehrlich S, Sponheim SR, Clark VP, Turner JA, Mueller BA, Magnotta V, O'Leary D, Ho BC, Brauns S, Manoach DS, Seidman L, Bustillo JR, Lauriello J, Bockholt J, Lim KO, Rosen BR, Schulz SC, Calhoun VD, Andreasen NC (2013): The MCIC collection: A shared repository of multi-modal, multi-site brain image data from a clinical investigation of schizophrenia. Neuroinformatics 11:367–388.

Guadalupe T, Zwiers MP, Teumer A, Wittfeld K, Vasquez AA, Hoogman M, Hagoort P, Fernandez G, Buitelaar J, Hegenscheid K, Volzke H, Franke B, Fisher SE, Grabe HJ, Francks C (2014): Measurement and genetics of human subcortical and hippocampal asymmetries in large datasets. Hum Brain Mapp 35:3277–3289.

Hamm HE (1998): The many faces of G protein signaling. J Biol Chem 273:669–672.

Hermans E, Challiss RAJ (2001): Structural, signalling and regulatory properties of the group I metabotropic glutamate receptors: Prototypic family C G-protein-coupled receptors. Biochem J 359:465–484.

Howie B, Fuchsberger C, Stephens M, Marchini J, Abecasis GR (2012): Fast and accurate genotype imputation in genome-wide association studies through pre-phasing. Nat Genet 44:955–959.

Koechlin E, Hyafil A (2007): Anterior prefrontal function and the limits of human decision-making. Science 318:594–598.

Koechlin E, Ody C, Kouneiher F (2003): The architecture of cognitive control in the human prefrontal cortex. Science 302:1181–1185.

Lancaster JL, Rainey LH, Summerlin JL, Freitas CS, Fox PT, Evans AC, Toga AW, Mazziotta JC (1997): Automated labeling of the human brain: A preliminary report on the development and evaluation of a forward-transform method. Hum Brain Mapp 5:238–242.

Lancaster JL, Woldorff MG, Parsons LM, Liotti M, Freitas CS, Rainey L, Kochunov PV, Nickerson D, Mikiten SA, Fox PT (2000): Automated Talairach atlas labels for functional brain mapping. Hum Brain Mapp 10:120–131.

Laureys S, Owen AM, Schiff ND (2004): Brain function in coma, vegetative state, and related disorders. Lancet Neurol 3:537–546.

Liang WS, Dunckley T, Beach TG, Grover A, Mastroeni D, Ramsey K, Caselli RJ, Kukull WA, McKeel D, Morris JC, Hulette CM, Schmechel D, Reiman EM, Rogers J, Stephan DA (2008): Altered neuronal gene expression in brain regions differentially affected by Alzheimer's disease: A reference data set. Physiol Genomics 33:240–256.

Lundstrom BN, Ingvar M, Petersson KM (2005): The role of precuneus and left inferior frontal cortex during source memory episodic retrieval. Neuroimage 27:824–834.

Lyuksyutova AI, Lu CC, Milanesio N, King LA, Guo NN, Wang YS, Nathans J, Tessier-Lavigne M, Zou YM (2003): Anterior–posterior guidance of commissural Axons by Wnt-frizzled signaling. Science 302:1984–1988.

Martin SJ, Grimwood PD, Morris RGM (2000): Synaptic plasticity and memory: An evaluation of the hypothesis. Annu Rev Neurosci 23:649–711.

Meigs TE, Fedor-Chaiken M, Kaplan DD, Brackenbury R, Casey PJ (2002): G alpha(12) and G alpha(13) negatively regulate the adhesive functions of cadherin. J Biol Chem 277:24594–24600.

Moers A, Nurnberg A, Goebbels S, Wettschureck N, Offermanns S (2008): G alpha(12)/G alpha(13) deficiency causes localized

overmigration of neurons in the developing cerebral and cerebellar cortices. Mol Cell Biol 28:1480–1488.

Nelson RJ, Demas GE, Huang PL, Fishman MC, Dawson VL, Dawson TM, Snyder SH (1995): Behavioral abnormalities in male-mice lacking neuronal nitric-oxide synthase. Nature 378: 383–386.

Neves SR, Ram PT, Iyengar R (2002): G protein pathways. Science 296:1636–1639.

Neves G, Cooke SF, Bliss TVP (2008): Synaptic plasticity, memory and the hippocampus: A neural network approach to causality. Nat Rev Neurosci 9:65–75.

Nurnberg A, Brauer AU, Wettschureck N, Offermanns S (2008): Antagonistic regulation of neurite morphology through G(q)/G(11) and G(12)/G(13). J Biol Chem 283:35526–35531.

Ochsner KN, Knierim K, Ludlow DH, Hanelin J, Ramachandran T, Glover G, Mackey SC (2004): Reflecting upon feelings: An fMRI study of neural systems supporting the attribution of emotion to self and other. J Cogn Neurosci 16:1746–1772.

Offermanns S (2001): In vivo functions of heterotrimeric G-proteins: Studies in G alpha-deficient mice. Oncogene 20:1635–1642.

Oldham WM, Hamm HE (2008): Heterotrimeric G protein activation by G-protein-coupled receptors. Nat Rev Mol Cell Biol 9: 60–71.

Peper JS, Brouwer RM, Boomsma DI, Kahn RS, Poll HEH (2007): Genetic influences on human brain structure: A review of brain imaging studies in twins. Hum Brain Mapp 28:464–473.

Polderman TJ, Benyamin B, de Leeuw CA, Sullivan PF, van Bochoven A, Visscher PM, Posthuma D (2015): Meta-analysis of the heritability of human traits based on fifty years of twin studies. Nat Genet 47:702–709.

Purcell S, Neale B, Todd-Brown K, Thomas L, Ferreira MA, Bender D, Maller J, Sklar P, de Bakker PI, Daly MJ, Sham PC (2007): PLINK: A tool set for whole-genome association and population-based linkage analyses. Am J Hum Genet 81:559–575.

Raz N, Rodrigue KM (2006): Differential aging of the brain: Patterns, cognitive correlates and modifiers. Neurosci Biobehav Rev 30:730–748.

Ripke S, Sanders AR, Kendler KS, Levinson DF, Sklar P, Holmans PA, Lin DY, Duan J, Ophoff RA, Andreassen OA, Scolnick E, Cichon S, Clair Corvin SD, Gurling A, Werge H, Rujescu T, Blackwood D, Pato DH, Malhotra CN, Purcell AK, Dudbridge S, Neale F, Rossin BM, Visscher L, Posthuma PM, Ruderfer D, Fanous DM, Stefansson A, Steinberg H, Mowry S, Golimbet BJ, V, Hert Jonsson DM, Bitter EG, Pietilainen I, Collier OP, Tosato DA, Agartz S, Albus I, Alexander M, Amdur M, Amin RL, Bass F, Bergen N, Black SE, Borglum DW, Brown AD, Bruggeman MA, Buccola R, Byerley NG, Cahn WF, Cantor W, Carr RM, Catts VJ, Choudhury SV, Cloninger K, Cormican CR, Craddock P, Danoy N, Datta PA, de Haan S, Demontis L, Dikeos D, Djurovic D, Donnelly S, Donohoe P, Duong G, Dwyer L, Fink-Jensen S, Freedman A, Freimer R, Friedl NB, Georgieva M, Giegling L, Gill I, Glenthoj M, Godard B, Hamshere S, Hansen M, Hansen M, Hartmann T, Henskens AM, Hougaard FA, Hultman DM, Ingason CM, Jablensky A, Jakobsen AV, Jay KD, Jurgens M, Kahn G, Keller RS, Kenis MC, Kenny G, Kim E, Kirov Y, Konnerth GK, Konte H, Krabbendam B, Krasucki L, Lasseter R, Laurent VK, Lawrence C, Lencz J, Lerer T, Liang FB, Lichtenstein KY, Lieberman P, Linszen JA, Lonnqvist DH, Loughland J, Maclean CM, Maher AW, Maier BS, Mallet W, Malloy J, Mattheisen P, Mattingsdal M, McGhee M, McGrath KA, McIntosh JJ, McLean A, McQuillin DE, Melle A, Michie I, Milanova PT, Morris V, Mors DW, Mortensen O, Moskvina PB, Muglia V, Myin-Germeys P, Nertney I, Nestadt DA, Nielsen G, Nikolov J, Nordentoft I, Norton M, Nothen N, O'Dushlaine MM, Olincy CT, Olsen A, O'Neill L, Orntoft FA, Owen TF, Pantelis MJ, Papadimitriou C, Pato G, Peltonen MT, Petursson L, Pickard H, Pimm B, Pulver J, Puri AE, Quested V, Quinn D, Rasmussen EM, Rethelyi HB, Ribble JM, Rietschel R, Riley M, Ruggeri BP, Schall M, Schulze U, Schwab TG, Scott SG, Shi RJ, Sigurdsson J, Silverman E, Spencer JM, Stefansson CC, Strange K, Strengman A, Stroup E, Suvisaari TS, Terenius J, Thirumalai L86. S, JH, Timm S, Toncheva D, van den Oord E, van Os J, van Winkel R, Veldink J, Walsh D, Wang AG, Wiersma D, Wildenauer DB, Williams HJ, Williams NM, Wormley B, Zammit S, Sullivan PF O'Donovan MC Daly MJ, Gejman PV (2011): Genome-wide association study identifies five new schizophrenia loci. Nat Genet 43:969–976.

Rissanen J (1978): Modeling by shortest data description. Automatica 14:465–471.

Sasaki T, Oga T, Nakagaki K, Sakai K, Sumida K, Hoshino K, Miyawaki I, Saito K, Suto F, Ichinohe N (2014): Developmental expression profiles of axon guidance signaling and the immune system in the marmoset cortex: Potential molecular mechanisms of pruning of dendritic spines during primate synapse formation in late infancy and prepuberty (I). Biochem Biophys Res Commun 444:302–306.

Shaw P, Greenstein D, Lerch J, Clasen L, Lenroot R, Gogtay N, Evans A, Rapoport J, Giedd J (2006): Intellectual ability and cortical development in children and adolescents. Nature 440: 676–679.

Sotelo C (2004): Cellular and genetic regulation of the development of the cerebellar system. Prog Neurobiol 72:295–339.

Sowell ER, Peterson BS, Thompson PM, Welcome SE, Henkenius AL, Toga AW (2003): Mapping cortical change across the human life span. Nat Neurosci 6:309–315.

Stein JL, Medland SE, Vasquez AA, Hibar DP, Senstad RE, Winkler AM, Toro R, Appel K, Bartecek R, Bergmann O, Bernard M, Brown AA, Cannon DM, Chakravarty MM, Christoforou A, Domin M, Grimm O, Hollinshead M, Holmes AJ, Homuth G, Hottenga JJ, Langan C, Lopez LM, Hansell NK, Hwang KS, Kim S, Laje G, Lee PH, Liu X, Loth E, Lourdusamy A, Mattingsdal M, Mohnke S, Maniega SM, Nho K, Nugent AC, O'Brien C, Papmeyer M, Putz B, Ramasamy A, Rasmussen J, Rijpkema M, Risacher SL, Roddey JC, Rose EJ, Ryten M, Shen L, Sprooten E, Strengman E, Teumer A, Trabzuni D, Turner J, van Eijk K, van Erp TG, van Tol MJ, Wittfeld K, Wolf C, Woudstra S, Aleman A, Alhusaini S, Almasy L, Binder EB, Brohawn DG, Cantor RM, Carless MA, Corvin A, Czisch M, Curran JE, Davies G, de Almeida MA, Delanty N, Depondt C, Duggirala R, Dyer TD, Erk S, Fagerness J, Fox PT, Freimer NB, Gill M, Goring HH, Hagler DJ, Hoehn D, Holsboer F, Hoogman M, Hosten N, Jahanshad N, Johnson MP, Kasperaviciute D, Kent JW Jr, Kochunov P, Lancaster JL, Lawrie SM, Liewald DC, Mandl R, Matarin M, Mattheisen M, Meisenzahl E, Melle I, Moses EK, Muhleisen TW, Nauck M, Nothen MM, Olvera RL, Pandolfo M, Pike GB, Puls R, Reinvang I, Renteria ME, Rietschel M, Roffman JL, Royle NA, Rujescu D, Savitz J, Schnack HG, Schnell K, Seiferth N, Smith C, Steen VM, Valdes Hernandez MC, Van den Heuvel M, van der Wee NJ, Van Haren NE, Veltman JA, Volzke H, Walker R, Westlye LT Whelan CD Agartz I,

Boomsma DI, Cavalleri GL, Dale AM, Djurovic S, Drevets WC, Hagoort P, Hall J, Heinz A, Jack CR Jr, Foroud TM, Le Hellard S, Macciardi F, Montgomery GW, Poline JB, Porteous DJ, Sisodiya SM, Starr JM, Sussmann J, Toga AW, Veltman DJ, Walter H, Weiner MW, Bis JC, Ikram MA, Smith AV, Gudnason V, Tzourio C, Vernooij MW, Launer LJ, DeCarli C, Seshadri S, Andreassen OA, Apostolova LG, Bastin ME, Blangero J, Brunner HG, Buckner RL, Cichon S, Coppola G, de Zubicaray GI, Deary IJ, Donohoe G, de Geus EJ, Espeseth T, Fernandez G, Glahn DC, Grabe HJ, Hardy J, Hulshoff Pol HE, Jenkinson M, Kahn RS, McDonald C, McIntosh AM, McMahon FJ, McMahon KL, Meyer-Lindenberg A, Morris DW, Muller-Myhsok B, Nichols TE, Ophoff RA, Paus T, Pausova Z, Penninx BW, Potkin SG, Samann PG, Saykin AJ, Schumann G, Smoller JW, Wardlaw JM, Weale ME, Martin NG, Franke B, Wright MJ, Thompson PM (2012): Identification of common variants associated with human hippocampal and intracranial volumes. Nat Genet 44:552–561.

Stranger BE, Stahl EA, Raj T (2011): Progress and promise of genome-wide association studies for human complex trait genetics. Genetics 187:367–383.

Tanaka S, Ishii K, Kasai K, Yoon SO, Saeki Y (2007): Neural expression of G protein-coupled receptors GPR3, GPR6, and GPR12 up-regulates cyclic AMP levels and promotes neurite outgrowth. J Biol Chem 282:10506–10515.

Thompson PM, Cannon TD, Narr KL, van Erp T, Poutanen VP, Huttunen M, Lonnqvist J, Standertskjold-Nordenstam CG, Kaprio J, Khaledy M, Dail R, Zoumalan CI, Toga AW (2001): Genetic influences on brain structure. Nat Neurosci 4:1253–1258.

Thompson PM, Stein JL, Medland SE, Hibar DP, Vasquez AA, Renteria ME, Toro R, Jahanshad N, Schumann G, Franke B, Wright MJ, Martin NG, Agartz I, Alda M, Alhusaini S, Almasy L, Almeida J, Alpert K, Andreasen NC, Andreassen OA, Apostolova LG, Appel K, Armstrong NJ, Aribisala B, Bastin ME, Bauer M, Bearden CE, Bergmann O, Binder EB, Blangero J, Bockholt HJ, Boen E, Bois C, Boomsma DI, Booth T, Bowman IJ, Bralten J, Brouwer RM, Brunner HG, Brohawn DG, Buckner RL, Buitelaar J, Bulayeva K, Bustillo JR, Calhoun VD, Cannon DM, Cantor RM, Carless MA, Caseras X, Cavalleri GL, Chakravarty MM, Chang KD, Ching CR, Christoforou A, Cichon S, Clark VP, Conrod P, Coppola G, Crespo-Facorro B, Curran JE, Czisch M, Deary IJ, de Geus EJ, den Braber A, Delvecchio G, Depondt C, de Haan L, de Zubicaray GI, Dima D, Dimitrova R, Djurovic S, Dong H, Donohoe G, Duggirala R, Dyer TD, Ehrlich S, Ekman CJ, Elvsashagen T, Emsell L, Erk S, Espeseth T, Fagerness J, Fears S, Fedko I, Fernandez G, Fisher SE, Foroud T, Fox PT, Francks C, Frangou S, Frey EM, Frodl T, Frouin V, Garavan H, Giddaluru S, Glahn DC, Godlewska B, Goldstein RZ, Gollub RL, Grabe HJ, Grimm O, Gruber O, Guadalupe T, Gur RE, Gur RC, Goring HH, Hagenaars S, Hajek T, Hall GB, Hall J, Hardy J, Hartman CA, Hass J, Hatton SN, Haukvik UK, Hegenscheid K, Heinz A, Hickie IB, Ho BC, Hoehn D, Hoekstra PJ, Hollinshead M, Holmes AJ, Homuth G, Hoogman M, Hong LE, Hosten N, Hottenga JJ, Hulshoff Pol HE, Hwang KS, Jack CR Jr, Jenkinson M, Johnston C, Jonsson EG, Kahn RS, Kasperaviciute D, Kelly S, Kim S, Kochunov P, Koenders L, Kramer B, Kwok JB, Lagopoulos J, Laje G, Landen M, Landman BA, Lauriello J, Lawrie SM, Lee PH, Le Hellard S, Lemaitre H, Leonardo CD, Li CS, Liberg B, Liewald DC, Liu X, Lopez LM, Loth E, Lourdusamy A, Luciano M, Macciardi F, Machielsen MW, Macqueen GM, Malt UF, Mandl R, Manoach DS, Martinot JL, Matarin M, Mather KA, Mattheisen M, Mattingsdal M, Meyer-Lindenberg A, McDonald C, McIntosh AM, McMahon FJ, McMahon KL, Meisenzahl E, Melle I, Milaneschi Y, Mohnke S, Montgomery GW, Morris DW, Moses EK, Mueller BA, Munoz Maniega S, Muhleisen TW, Muller-Myhsok B, Mwangi B, Nauck M, Nho K, Nichols TE, Nilsson LG, Nugent AC, Nyberg L, Olvera RL, Oosterlaan J, Ophoff RA, Pandolfo M, Papalampropoulou-Tsiridou M, Papmeyer M, Paus T, Pausova Z, Pearlson GD, Penninx BW, Peterson CP, Pfennig A, Phillips M, Pike GB, Poline JB, Potkin SG, Putz B, Ramasamy A, Rasmussen J, Rietschel M, Rijpkema M, Risacher SL, Roffman JL, Roiz-Santianez R, Romanczuk-Seiferth N, Rose EJ, Royle NA, Rujescu D, Ryten M, Sachdev PS, Salami A, Satterthwaite TD, Savitz J, Saykin AJ, Scanlon C, Schmaal L, Schnack HG, Schork AJ, Schulz SC, Schur R, Seidman L, Shen L, Shoemaker JM, Simmons A, Sisodiya SM, Smith C, Smoller JW, Soares JC, Sponheim SR, Sprooten E, Starr JM, Steen VM, Strakowski S, Strike L, Sussmann J, Samann PG, Teumer A, Toga AW, Tordesillas-Gutierrez D, Trabzuni D, Trost S, Turner J, Van den Heuvel M, van der Wee NJ, van Eijk K, van Erp TG, van Haren NE, van't Ent D, van Tol MJ, Valdes Hernandez MC, Veltman DJ, Versace A, Volzke H, Walker R, Walter H, Wang L, Wardlaw JM, Weale ME, Weiner MW, Wen W, Westlye LT, Whalley HC, Whelan CD, White T, Winkler AM, Wittfeld K, Woldehawariat G, Wolf C, Zilles D, Zwiers MP, Thalamuthu A, Schofield PR, Freimer NB, Lawrence NS, Drevets W; the Alzheimer's Disease Neuroimaging Initiative ECICSYSG (2014): The ENIGMA Consortium: Large-scale collaborative analyses of neuroimaging and genetic data. Brain Imaging Behav 8:153–182.

Winkler AM, Kochunov P, Blangero J, Almasy L, Zilles K, Fox PT, Duggirala R, Glahn DC (2010): Cortical thickness or grey matter volume? The importance of selecting the phenotype for imaging genetics studies. Neuroimage 53:1135–1146.

Xu L, Groth KM, Pearlson G, Schretlen DJ, Calhoun VD (2009): Source-based morphometry: The use of independent component analysis to identify gray matter differences with application to schizophrenia. Hum Brain Mapp 30:711–724.

Yang JA, Lee SH, Goddard ME, Visscher PM (2011): GCTA: A tool for genome-wide complex trait analysis. Am J Hum Genet 88:76–82.

Zhang JH, Pandey M, Seigneur EM, Panicker LM, Koo L, Schwartz OM, Chen WP, Chen CK, Simonds WF (2011): Knockout of G protein beta 5 impairs brain development and causes multiple neurologic abnormalities in mice. J Neurochem 119:544–554.

Zhou L, Zhu DY (2009): Neuronal nitric oxide synthase: Structure, subcellular localization, regulation, and clinical implications. Nitric Oxide-Biol Chem 20:223–230.